Accepted Manuscript

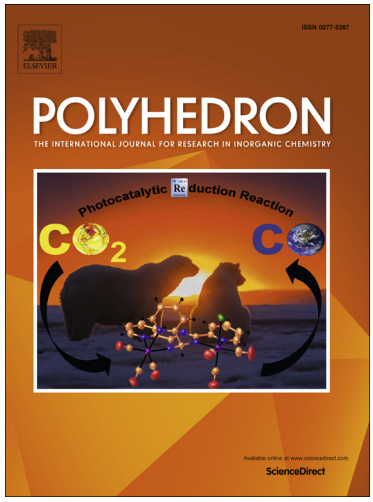

Antibacterial and catecholase activities of Co(III) and Ni(II) Schiff base complexes

Ayon Kanti Ghosh, Merry Mitra, Aafreen Fathima, Hareram Yadav, Angshuman Roy Choudhury, Balachandran Unni Nair, Rajarshi Ghosh

PII: S0277-5387(16)00019-X
DOI: http://dx.doi.org/10.1016/j.poly.2016.01.015
Reference: POLY 11777

To appear in: *Polyhedron*

Received Date: 29 September 2015
Accepted Date: 7 January 2016

Please cite this article as: A.K. Ghosh, M. Mitra, A. Fathima, H. Yadav, A.R. Choudhury, B.U. Nair, R. Ghosh, Antibacterial and catecholase activities of Co(III) and Ni(II) Schiff base complexes, *Polyhedron* (2016), doi: http://dx.doi.org/10.1016/j.poly.2016.01.015

Antibacterial and catecholase activities of Co(III) and Ni(II) Schiff base complexes

Ayon Kanti Ghosh[a], Merry Mitra[a], Aafreen Fathima[b], Hareram Yadav[c], Angshuman Roy Choudhury[c], Balachandran Unni Nair[b,*], Rajarshi Ghosh[a,*]

[a]Department of Chemistry, The University of Burdwan, Burdwan 713 104, India

[b]Chemical Laboratory, Central Leather Research Institute, Adyar, Chennai 600 020, India

[c]Department of Chemical Sciences, Indian Institute of Science Education & Research, Mohali, Sector 81, S.A.S. Nagar, Knowledge City, Manauli PO, Mohali 140 306, India

Abstract

X-ray structural analyses of two newly synthesized Schiff base-complexes, $[Co(L)_3]$ (**1**) and $[Ni(L)_2]$ (**2**) [HL = 2-((*E*)-(2-pyridine-2-pyridin-2-ylthio)ethylimino)methyl)phenol], reveal the bidentate chelation behavior of the ligand HL with octahedral and square planar geometries at the metal centers in **1** and **2**, respectively. Both the compounds show antibacterial activity as well as catecholase activity. The antibacterial activities of the compounds were investigated on gram positive and gram negative bacteria; compound **2** was found to be better in terms of antibacterial activity than **1** against both the bacteria.

Moreover, both compounds catalyse the oxidation of 3,5-ditertiarybutylcatechol in methanol in the presence of molecular oxygen with first order reaction kinetics and turn over numbers 3.48×10^3 h^{-1} (**1**) and 2.68×10^3 h^{-1} (**2**).

Keyword: Cobalt, Nickel, Schiff base, Antibacterial activity, Catecholase activity

_____

*Corresponding author, E. mail: rghosh@chem.buruniv.ac.in

1. Introduction

The synthesis and characterization of coordination complexes are presently of increased interest because of their potential application in catalysis [1], adsorption [2], storage [3], magnetism [4], molecular recognition [5], fluorescence [6], sensors [7], etc. Judicious choice of the metal ions and ligands often makes molecules multifunctional instead of showing a single property [8]. Transition metals having different geometries and oxidation numbers, and synthetically easy accessible Schiff bases with varied denticities may be used for this purpose. As organic imines are successful intermediates in synthesizing different biologically active organic molecules and pharmaceutical substances [9], here we have synthesized and characterized one nickel(II) and one cobalt(III) complex of a newly synthesized (N,S,O) donor Schiff base ligand, 2-((*E*)-(2-pyridine-2-pyridin-2-

ylthio)ethylimino)methyl)phenol (HL), having one imine group, though in each complex the ligand binds with the metal ions using its (N,O) donor sites.

Coordination compound models of the active sites of enzymes, which are capable of processing molecular oxygen under ambient conditions, have received a great deal of attention [10] as they can serve as efficient catalysts for synthetic transformations of industrial importance [11]. Hence modelling coordination compounds of metalloenzymes with oxidase (oxygenase) activity in particular are very important for the development of bioinspired catalysts for oxidation reactions [12]. In parallel, designing synthetic coordination compounds with better antimicrobial activity than the commercially available antibiotics is also of immense importance in medicinal chemistry [13,14].

In this present endeavor, our newly synthesized Schiff base-complexes $[Co(L)_3]$ (**1**) and $[Ni(L)_2]$ (**2**) show more than one function, such as antimicrobial and catecholase activity. In addition to the activity of the complexes against microbes, each of these serves as models for the plant enzyme catecholase and hence catalyses the oxidation of 3,5-ditertiarybutyl catechol (3,5-DTBC) to 3,5-ditertiarybutyl quinone (3,5-DTBQ) in the presence of aerial oxygen.

2. Experimental

2.1. Materials

2-Mercaptopyridine, 2-chloroethylamine and salicyaldehyde were purchased from Sigma Aldrich and used as received. Cobalt(II) acetate tetrahydrate and nickel(II) acetate tetrahydrate were purchased from E. Merck India. Solvents were of reagent grade and used without further purification.

The gram positive bacteria *Bacillus subtilis* was received from the biotechnology department of Indian Institute of Technology Madras (IITM) and *E.coli MTCC 40* gram negative bacteria was procured from the Microbial type culture collection (*MTCC*), Chandigarh, India. Growth media, such as Nutrient agar and Nutrient broth, were obtained from Hi-Media (Mumbai, India). The antibiotic discs and sterile filter paper discs were obtained from Hi-Media (Mumbai, India). All other chemicals used were of analytical grade procured from SD Fine chemicals, India.

2.2. Physical measurements

Elemental analyses (carbon, hydrogen and nitrogen) were performed on a Perkin-Elmer 2400 CHNS/O elemental analyzer. UV-VIS and IR spectra (KBr discs, 4000-300 cm^{-1}) were recorded using a Shimadzu UV-VIS 2450 spectrophotometer and Perkin-Elmer FT-IR model RX1 spectrometer, respectively.

2.3. Zone of inhibition by the Agar diffusion method

The antibacterial activity was measured by the Kirby Bauer disc diffusion method [15] against gram positive bacteria (*Bacillus Subtilis*) and gram negative bacteria (*E.coli MTCC 40*). An overnight culture adjusted to 0.5 Mac Farland turbidity was used for swabbing nutrient agar plates (comprising of 3 g/l meat extract, 5 g/l peptic digest of animal tissue and 15 g/l of agar) to do a lawn culture of the test bacterium. Then using sterile forceps, plain filter paper discs and antibiotic loaded discs were placed onto the agar plates. 20 µl of varying concentrations (0.1, 1 and 2.5 µg/disc) of test sample were loaded over the filter paper discs. The plates were incubated at 37º C for 24 h and observed for the zone of inhibition around the discs. Commercial antibiotics such as Ampicillin and Cephotaxime were used as standards for comparison.

2.4. Minimum Inhibitory Concentration (MIC)

The MIC was carried out at different concentrations ranging from 100, 50, 25 to 1.56 µg/ml using nutrient broth (Comprising of 5 g/l peptone, 1.5 g/l beef extract, 1.5 g/l yeast extract, 5g/l NaCl) by the broth dilution method [16]. The tubes containing the growth medium were serially diluted with the test sample, followed by the addition of a bacterial inoculum of 0.5 Mac Farland turbidity. The tubes were incubated at 37º C for 24 h and the MIC's were recorded as the tube showing no visible growth after comparing with the positive controls.

2.5. Minimum Bactericidal Concentration (MBC)

The MBC (Minimum Bactericidal Concentration) was determined by spot inoculating a nutrient agar plate with the same tubes used for the MIC measurements, having varying concentrations of the test sample. The nutrient agar plates were incubated at 37 °C for 24 h and the MBC was recorded as the lowest concentration of the test sample which did not produce any bacterial growth on the nutrient agar medium [17].

2.6. Time kill assay

A time kill assay for the test sample was carried out by the modified plating technique [18]. To tubes containing 8 ml of nutrient broth, 1 ml of the test sample of MIC and 2 x MIC concentration was incorporated, followed by 1 ml of bacterial inoculum, so that the overall volume of the tubes was 10 ml. The tubes, along with the controls, were incubated at 37 °C with moderate shaking in an orbital shaker. Samples were collected after 0, 4, 8 and 12 h incubation to determine the cfu/ml by the plate count technique.

2.7. Synthesis of HL

The ligand's synthesis is depicted in Scheme 1. 2-Mercaptopyridine (8 mmol, 0.88 g) was added gradually to a sodium ethoxide solution with continuous stirring. Then 2-chloroethylamine (8 mmol, 0.63 g) was mixed slowly to this reaction mixture and the mixture was stirred for about 1 hour. During this stirring precipitation of sodium chloride confirms the formation of 2-(pyridin-2-ylthio)ethanamine (Scheme 1). This product was characterized by ^{1}H NMR. Sodium chloride was separated by filtration. Addition of salicyaldehyde (8 mmol, 0.97 g) to this solution of 2-(pyridin-2-ylthio)ethanamine with a four hour reflux gives the ligand HL.

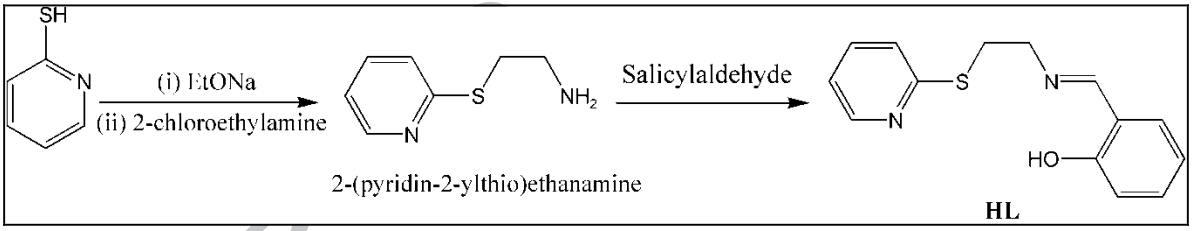

Scheme 1

Yield (2-(pyridin-2-ylthio)ethanamine): 0.98 g (80%). Anal cal. for $C_7H_{10}N_2S$: C, 54.51; H, 6.54; N, 18.17; Found: C, 54.01; H, 6.21; N, 18.20%. IR (KBr pellet, cm^{-1}): 756, 1557, 1576. UV-Vis (λ, nm, MeOH): 248 ($\varepsilon = 6.51 \times 10^3$), 287 ($\varepsilon = 4.81 \times 10^3$), 359 ($\varepsilon = 1.05 \times 10^3$) ^{1}H NMR δ (ppm): 2.11 (bs, 2H), 2.99 (t, J = 6.4 Hz, 2H), 3.28 (t, J = 6.4 Hz, 2H), 4.50 (bs, 2H), 6.95-6.98 (m, 1H), 7.18 (d,

J = 8.0 Hz, 1H), 7.44-7.48 (m, 1H), 8.40 (d, J = 4.8 Hz, 1H) (Fig. S1, Supporting Information).

Yield (HL): 1.15 g (70%). Anal cal. for $C_{14}H_{14}N_2SO$: C, 65.08; H, 5.46; N, 10.84; Found: C, 65.01; H, 5.11; N, 10.91%. IR (KBr pellet, cm^{-1}): 757, 1557, 1574, 1626. UV-Vis (λ, nm, MeOH): 213 ($\varepsilon = 1.70 \times 10^4$), 251 ($\varepsilon = 1.23 \times 10^4$), 289 ($\varepsilon = 4.60 \times 10^3$), 402 ($\varepsilon = 5.57 \times 10^2$). ^{1}H NMR δ (ppm): 3.51 (t, J = 6.4 Hz, 2H), 3.91 (td, J = 6.4, 0.8 Hz, 2H), 6.85 (td, J = 7.6, 0.8 Hz, 1H), 6.94-6.98 (m, 2H), 7.16 (dd, J = 8.4, 0.8 Hz, 1H), 7.23 (dd, J = 7.6, 1.6 Hz, 2H), 7.27-7.31 (m, 1H), 7.44 (td, J = 7.6, 1.6 Hz, 1H), 8.34 (s, 1H), 8.41-8.43 (m, 1H), 13.32 (bs, 1H) (Fig. S2, Supporting Information)

*2.8. Synthesis of compound **1***

Solid cobalt(II) acetate tetrahydrate (0.1 mmol, 0.02 g) was slowly added to a stirring solution of HL (0.1 mmol, 0.02 g) in ethanol. The mixture was stirred with a little warming until all the cobalt(II) salt was dissolved. The brown colour of the ligand solution intensified on dissolution of the metal salt. Brown coloured X-ray quality crystals of **1** appeared after keeping the solution in the open air after a week or so.

Yield: 0.04 g (60%). Anal cal. for $C_{42}H_{39}N_6S_3O_3Co$: C, 60.71; H, 4.73; N, 10.11; Found: C, 60.59; H, 4.68; N, 10.21%. IR (KBr pellet, cm^{-1}): 750, 1576, 1609. UV-Vis (λ, nm, MeOH): 250, 390, 600.

2.9. Synthesis of Compound ***2***

An ethanolic solution of nickel(II) acetate tetrahydrate (0.1 mmol, 0.02 g) was added dropwise to the ligand HL (0.1 mmol, 0.25 g) in ethanol with gentle stirring. The brown coloured ligand solution changed to light green. The reaction mixture was kept in the open air. After 2 days green coloured block shaped crystals of **2** appeared.

Yield: 0.0315 g (55%). Anal cal. for $C_{28}H_{26}N_4S_2O_2Ni$: C, 58.66; H, 4.57; N, 9.77; Found: C, 58.50; H, 4.51; N, 9.91%. IR (KBr pellet, cm^{-1}): 3452, 1608, 756. UV-Vis (λ, nm, MeOH): 218, 244, 372, 610.

2.10. X-ray diffraction study

Single crystal X-ray diffraction data were collected using a RigakuXtaLABmini diffractometer equipped with a Mercury CCD detector. The data were collected with graphite monochromated Mo-Kα radiation (λ = 0.71073 Å) at 100 K using ω scans. The data were reduced using Crystal Clear suite 2.0 [19] and the space group determination was done using Olex2 [20]. The structure was resolved by direct methods and refined by full-matrix least-squares procedures using the SHELXL [21] package with the OLEX2 suite. The crystal data and

refinement details are listed in Table 1. All the figures have been generated using ORTEP-32 [22].

3. Results and discussion

3.1. Synthesis of the ligand and the complexes

The ligand HL was synthesized in two steps. Initially 2-mercaptopyridine was refluxed with 2-chloroethylamine in dry ethanol in the presence of sodium ethoxide to produce 2-(pyridin-2-ylthio)ethanamine. The organic product was extracted and the solvent was evaporated as a yellow solid. This was characterized using spectroscopic tools. 2-(Pyridin-2-ylthio)ethanamine was further refluxed with salicyalidehyde to synthesize HL. In the IR spectrum of HL, the band at 756 cm^{-1} was assigned as a υ_{C-S} stretching frequency, whereas bands at 1557 and 1576 cm^{-1} are due to asymmetric $\upsilon_{C=N}$ frequencies. The ^1H NMR spectrum of 2-(pyridin-2-ylthio)ethanamine in $CDCl_3$ showed the characteristic peaks of the protons. The signals of the amine protons of 2-(pyridin-2-ylthio)ethanamine were at the δ 2.11 ppm (bs, 2H). Two triplet signals for the four protons of the two methylene groups were observed at δ 2.99 ppm (t, J = 6.4 Hz, 2H) for one methylene group α to the NH_2 group and δ 3.28 ppm (t, J = 6.4 Hz, 2H) for that β to the amine group. The signals of the three aromatic protons were found at different δ values, namely 6.95-6.98 (m, 1H), 7.18 (d, J = 8.0 Hz, 1H) and 7.44-7.48 ppm (m, 1H). One doublet

signal in the deshielded region, at δ 8.48 ppm (d, J = 4.8 Hz, 1H) is attributable to the proton in an *ortho* position to the pyridine N atom. The ^{1}H NMR spectrum of HL in $CDCl_3$ also showed the characteristic peaks of the protons. The two peaks at δ 3.51 ppm (t, J = 6.4 Hz, 2H) for one methylene group α to the NH_2 group and δ 3.91 ppm (td, J = 6.4 , 0.8 Hz, 2H) for another β to the amine group were shifted downfield after condensation. The imine proton was confirmed by a peak appearing at δ 8.34 ppm (s, 1H). The peaks for the aromatic protons in the *ortho* position to the pyridine N atom were observed at δ 8.41-8.43 ppm (m, 1H). The disappearance of the amine peak at δ 2.11, the simultaneous downfield shift of two methylene peaks and the formation of an imine proton peak at δ 8.34 ppm proves the formation of the imine bond.

Compounds **1** and **2** were synthesized in good yield mixing the metal(II) acetates with the ligand HL in methanol at room temperature. In the IR spectra of the complexes the bands at ~1576-1609 cm^{-1} were attributed to the asymmetric $\upsilon_{C=N}$ stretching and the band at ~750 cm^{-1} was detected for the υ_{C-S} stretching.

3.2. X-ray structures

Thermal plots of **1** and **2** are given in Figs. 1 and 2, respectively. From the bond angle and bond distance data (Table 2), the geometry around the Co(III) ion can be described as a distorted octahedron with a *meridional* conformation. Four of

the three coordination sites in the horizontal plane of the octahedron are occupied by the imine nitrogen atoms (N1, N2 and N3) of the Schiff base. The remaining position in the octahedral horizontal plane is occupied by the phenoxo oxygen atom (O1) of the ligand framework. The other two phenoxo oxygen atoms (O2 and O3) are placed in the axial positions. The bond distances in the horizontal plane are in the range 1.882(3)-1.962(3) Å. The dihedral angle between the planes containing the two rings of each ligand in **1** comprising the atoms N4-C10-C11-C14-C13-C12 and C7-C6-C2-C3-C4-C5 is 41.30°, that of N6-C38-C39-C40-C41-C42 and C35-C31-C30-C32-C33-C34 is 42.36° and that of N5-C24-C28-C25-C26-C27 and C21-C16-C19-C17-C20-C18 is 53.97°.

In the same way, considering the bond angle and bond distance data (Table 3), the coordination environment around the Ni(II) ion is best described as a distorted square planar geometry with the imine nitrogen atoms (N1 and N1') and phenoxo oxygen atoms (O1 and O1') in mutually *trans* positions. The dihedral angle between the planes containing the two rings of each ligand in **2** comprising the atoms N2-C10-C11-C12-C14-C13 and C1-C6-C5-C3-C2-C4 is 81.87°.

3.3. Antibacterial activity

The antibacterial activity of the ligand (HL) and compound **1** was measured by the Kirby Bauer disc diffusion method against gram positive bacteria (*Bacillus*

Subtilis) and gram negative bacteria (*E.coli MTCC 40*). The concentrations of the compounds tested were 0.1, 1 and 2.5 μg/disc. For standards, two commercial antibiotics were used, namely Cephotaxime – Ce^{10} and Ampicillin – AMP^{10} (Tables 4 and 5).

The zone of inhibitions for the maximum concentration (2.5 μg/disc) tested against *Bacillus subtilis* and *E. coli* were found to be 13 and 12 mm, respectively for HL and 12 and 10 mm, respectively for **1**. The respective minimum inhibitory concentration (MIC) results for *Bacillus subtilis* and *E.coli* were found to be 50 and 100 μg/ml. The minimum bacterial concentration (MBC) results for both HL and **1** for *E.coli* were undetermined as the concentrations tested against *E.coli* were not able to inhibit the growth of the bacteria even at 100 μg/ml, whereas for *Bacillus subtilis* the MBC was found to be 100 μg/ml.

From the rate of kill assay results (for **1**) it could be concluded that the compound does not possess profound bactericidal activity for *Bacillus subtilis* and *E.coli*, even at 2 × MIC concentration. The time kill assay data is presented in terms of $\log_{10}$ cfu/ml in Table 6. The difference in the antibacterial activity might be due to the type and composition of the bacterial cell wall as well as membrane permeabilization, which is why upon comparison the compound shows fair activity against gram positive bacteria (*Bacillus subtilis*) and was not active against gram negative bacteria (*E.coli*) [23].

The antibacterial activity of compound **2** was studied by the Agar disc diffusion method and it was found that out of the three concentrations tested the compound showed better inhibition at a concentration of 2.5 µg/ 20 µl for *Bacillus subtilis*, with an inhibition zone of 15.5 mm, as compared to *E.coli*, which showed 10.25 mm as the zone of inhibition for the same concentration tested (Table 7). To determine the minimum amount of sample required to inhibit the bacterial growth, the MIC was measured and it was found that out of the various concentrations tested (100, 50, 25, 12.5, 6.25, 3.12, 1.56 µg/ml), the growth of *Bacillus subtilis* was inhibited at 12.5 µg/ ml, whereas the growth of *E.coli* was inhibited at 25 µg/ml. The MBC values were found to be 25 µg/ml for *Bacillus subtilis* and 50 µg/ml for *E.coli*.

In this study compound **2** was found to be more active towards gram positive bacteria, *Bacillus subtilis*. The reason for this might be differences in the bacterial cell wall composition and its thickness, as gram negative bacteria have an extra layer of lipopolysaccharide (LPS) [24]. The permeability barrier of the cell membranes also plays an important role in allowing the penetration of the antibacterial agent [23]. From the rate of kill assay results it could be concluded, after comparing the reduction in viable cell count, that the compound was found to be bactericidal for *Bacillus subtilis* at 2 × MIC concentration (25 µg/ml), showing no growth or colony formation. For *E. coli* the compound showed no significant

bactericidal activity at the MIC (25 μg/ml) or at 2 × MIC (50 μg/ml) concentration. The time kill assay data is presented in terms of log10 cfu/ml in Table 8. The difference in the antibacterial activity might be due to the type and composition of the bacterial cell wall as well as membrane permeabilization which is why the compound shows better activity against gram positive bacteria (*Bacillus subtilis*) than gram negative bacteria (*E.coli*) [23].

*3.4. Catecholase activity of **1** and **2**: spectrophotometric study*

For the study of the catecholase activity of complexes **1** and **2**, 3,5-DTBC, with two bulky *t*-butyl substituents on the ring and a low quinone-catechol reduction potential, has been chosen as the substrate. This makes it easily oxidizable to the corresponding *o*-quinone, 3,5-DTBQ, which is highly stable and shows a maximum absorption at 401 nm in methanol. Solutions of **1** and **2** were treated with 100 equivalents of 3,5-DTBC under aerobic conditions. Repetitive UV-Vis spectral scans for both complexes were recorded in pure MeOH (Figs. 3 and 4). Spectral bands at 250, 390 and 600, and 218, 244, 372 and 610 nm appeared in the electronic spectra of complexes **1** and **2**, respectively whereas 3,5-DTBC shows a single band at 282 nm. After addition of 3,5-DTBC, the time dependent spectral scans show a very smooth growth of the quinone band at 401 nm, as reported by Krebs *et al* [25], concomitant with a decrease in the

characteristic 282 nm band for 3,5-DTBC, which indicates the formation of the respective quinone derivative, 3,5-DTBQ, that was subsequently purified by column chromatography. The product was isolated in high yield (71.1 and 75.8% for **1** and **2**, respectively) by slow evaporation of the eluant and was identified by ^{1}H NMR spectroscopy (Figs. S3 and S4; Supporting information). ^{1}H NMR ($CDCl_3$, 400 MHz) for **1**, δ_H (ppm): 1.22 (s, 9H), 1.26 (s, 9H), 6.21 (d, J = 2.4 Hz, 1H), 6.93 (d, J = 2.0 Hz, 1H). For **2**, δ_H (ppm): 1.16 (s, 9H), 1.20 (s, 9H), 6.15 (d, J = 2.4 Hz, 1H), 6.86 (d, J = 2.4 Hz, 1H).

To find out the comparative reaction velocity between 3,5-DTBC and the complexes, the reaction kinetics between the complexes and 3,5-DTBC was studied by observing the time dependent change in absorbance at a wavelength of 401 nm, which is characteristic of 3,5-DTBQ in methanol. The colour of the solution gradually turned deep brown, indicative of the gradual conversion of 3,5-DTBC to 3,5-DTBQ. The difference in absorbance ΔA at 401 nm, was plotted against time to obtain the velocity for that particular catalyst to substrate concentration ratio (Figs. 5 and 6). An overall first-order catalytic reaction was observed in the slowest rate-determining step, with velocities 2.54×10^{-3} and 2.77×10^{-3} min^{-1} for **1** and **2** respectively. Both the reactions are zero order with respect to O_2 (Figs. S5 and S6; Supporting information). The overall rate constants (k_{obs})

are 0.02341 min^{-1} for **1** and 0.02345 min^{-1} for **2** (Figs. S7 and S8; Supporting information).

3.5. Enzyme kinetics study

Enzymatic kinetic experiments were performed UV-Vis spectrophotometrically, thermostated at 25 °C, using complex **1** and **2** with the substrate 3,5-DTBC in MeOH. 0.04 ml of each complex solution, with a constant concentration of 1×10^{-4} M, was added to 2 ml of 3,5-DTBC of a particular concentration (varying its concentration from 1×10^{-3} to 1×10^{-2} M) to achieve an ultimate concentration of the complex of 1×10^{-4} M. The conversion of 3,-5-DTBC to 3,5-DTBQ was monitored with time at a wavelength of 401 nm for solutions in MeOH. The rate for each concentration of the substrate was determined by the initial rate method.

The rate versus concentration of substrate data were analyzed on the basis of the Michaelis-Menten approach of enzymatic kinetics to get the Lineweaver-Burk (double reciprocal) plot as well as the values of various kinetic parameters, namely V_{max}, K_M and K_{cat}. The observed rate vs. [substrate] plot in methanol solution, as well as the Lineweaver-Burk plot, is given in Figs. 7 and 8 for **1** and **2** respectively. The kinetic parameters are listed in Table 9. The turnover numbers (K_{cat}) are 3.48×10^3 (**1**) and 2.68×10^3 h^{-1} (**2**).

3.6. Mechanism of catecholase activity

In order to obtain a mechanistic inference of the catecholase activity and to get an idea about the complex-substrate intermediate, we recorded the ESI-MS spectrum (Figs. S9a and S9b; Supporting Information) of a 1:100 mixture of complex **1** and 3,5-DTBC. The protonated complex $[Co(L)_3H]^+$ exhibits a peak at m/z = 831. From the ESI-MS analysis we can predict that there is a detachment of a ligand moiety from the complex, which is evident from an m/z peak at 574 for the species $[Co(L)_2]^+$. Further detachment of the ligand is confirmed by a peak at m/z = 316 due to the formation of $[Co(L)]^{2+}$. The peak at m/z = 243 can be assigned to a sodium aggregate of quinone $[3,5\text{-DTBQ-Na}]^+$. The intermediate Co(II) species $[Co(L)_2(dtbq)_2]$ (Scheme S1, Supporting Information) is identified by a peak at m/z = 1015. The Co(III) complex is reduced to Co(II) in the intermediate state and 3,5-DTBC is oxidised to quinone in the presence of molecular oxygen.

Similarly, we recorded the ESI-MS spectrum (Figs. S10a and S10b; Supporting Information) of a 1:100 mixture of complex **2** and 3,5-DTBC. The signal at m/z = 259 is due to the formation of the protonated ligand $[(HL)H]^+$. The protonated complex $[Ni(L)_2H]^+$ exhibits a peak at m/z = 573. The peak at m/z = 243 can be assigned to a sodium aggregate of quinone $[3,5\text{-DTBQ-Na}]^+$. We can

also predict here that there is a detachment of a ligand moiety from the complex $[Ni(L)_2]$. This is evident from the m/z peak at 315 for the species $[Ni(L)]^+$. Formation of a sodium aggregate of the intermediate species [Ni(L)(DTBC)Na] (Scheme S2; Supporting Information) is identified by a peak at m/z = 558. The molecular oxygen that takes part in both oxidation processes for complexes **1** and **2** is converted to H_2O_2. The liberated H_2O_2 is identified and characterized spectrophotometrically (Fig. S11; Supporting Information) [26].

4. Conclusions

We have designed and synthesized two new compounds, $[Co(L)_3]$ (**1**) and $[Ni(L)_2]$ (**2**), which show antibacterial and catecholase activities. The antibacterial activities of both compounds, along with the ligand, were investigated on gram positive (*Bacillus subtilis*) and gram negative bacteria (*E.coli*). Compound **2** was found to be more active against *Bacillus subtilis* than *E.coli*, whereas compound **1** showed fair activity against *Bacillus subtilis* and was inactive against *E.coli*. The overall comparison of the compounds based on antibacterial activity suggests compound **1** is more active against both the bacteria than compound **2**. In parallel, the compounds show activity in catalyzing the oxidation of 3,5-ditertiarybutylcatechol to 3,5-ditertiarybutylquinone in methanol solvent in the presence of molecular oxygen. The reactions follow first order kinetics with

reaction rates of 2.54×10^{-3} and 2.77×10^{-3} min^{-1}, respectively. From the Michaelis-Menten reaction kinetics, the turnover numbers are calculated as 3.48×10^3 (**1**) and 2.68×10^3 h^{-1} (**2**).

5. Supplementary data

CCDC 1415640 (**1**) and 1415641 (**2**) contain the supplementary crystallographic data for **1** and **2**. This data can be obtained free of charge via http://www.ccdc.cam.ac.uk/conts/retrieving.html, or from the Cambridge Crystallographic Data Centre, 12 Union Road, Cambridge CB2 1EZ, UK; fax: (+44) 1223-336-033; or e-mail: deposit@ccdc.cam.ac.uk.

6. Acknowledgements

RG sincerely thanks the Department of Science & Technology, Government of West Bengal [No. 781(Sanc.)/ST/P/S&T/4G-4/2013 dated 04-12-2014] for financial assistance. AKG and MM thank CSIR, New Delhi and The University of Burdwan, respectively for their fellowships.

References

[1] (a) M. Shyamal, T. K. Mandal, A. Panja, A. Saha, RSC. Adv. 4 (2014) 53520-53530; (b) M. Das, R. Nasani, M. Saha, S. M. Mobin, S. Mukhopadhyay, Dalton Trans. 44 (2015) 2299-2310; (c) P. Kar, Y. Ida, T. Kanetomo, M. G. B. Drew, T. Ishida, A. Ghosh, Dalton Trans. 44 (2015) 9795-9804; (d) I. Majumder, P. Chakraborty, S. Das, H. Kara, S. K. Chattopadhyay, E. Zangrando, D. Das, RSC Adv. 5 (2015) 51290-51301.

[2] (a) H. -H. Zou, Y. -P. He, L. -C. Gui, F. -P. Liang, CrystEngComm. 13 (2011) 3325-3329; (b) C. J. Cramer, D. G. Truhlar, Phys. Chem. Chem. Phys. 11 (2009) 10757-10816; (c) S. Chakraborty, J. Zhang, Y. J. Patel, J. A. Krause, H. Guan, Inorg. Chem. 52 (2013) 37−47; (d) C. Lamberti, A. Zecchina, E. Groppo, S. Bordiga, Chem. Soc. Rev. 39 (2010) 4951-5001.

[3] (a) E. D. Bloch, W. L. Queen, R. Krishna, J. M. Zadrozny1, C. M. Brown, J. R. Long, Science 335 (2012) 1606-1610; (b) Y. -X. Tan, Y. -P. He, J. Zhang, Chem. Commun. 47 (2011) 10647-10649; (c) J. G. Vitillo, RSC Adv. 5 (2015) 36192-36239.

[4] (a) J. Kan, H. Wang, W. Sun, W. Cao, J. Tao, J. Jiang, Inorg. Chem. 52 (2013) 8505-8510; (b) A. Venugopal, F. Tuna, T. P. Spaniol, L. Ungur, L. F. Chibotaru, J. Okuda, R. A. Layfield, Chem. Commun. 49 (2013) 901-903; (c) I. -R. Jeon, R. Clérac, Dalton Trans. 41 (2012) 9569-9586.

[5] V. Madhu, S. Sabbani, R. Kishore, I. K. Naik, S. K. Das, CrystEngComm. 17 (2015) 3219-3223.

[6] (a) Z. -G. Gu , Y. -T. Liu , X. -J. Hong , Q. -G. Zhan , Z. -P. Zheng , S. -R. Zheng , W. -S. Li, S. -J. Hu , Y. -P. Cai, Cryst. Growth Des. 12 (2012) 2178–2186; (b) G. -Y. Wang, L. -L. Yang, Y. Li, H. Song, W. -J. Ruan, Z. Chang, X. -H. Bu, Dalton Trans. 42 (2013) 12865-12868.

[7] (a) T. Wen, D. -X. Zhang, J. Liu, R. Lin, J. Zhang, Chem. Commun. 49 (2013) 5660-5662; (b) H. Pang, F. Gao, Q. Chen, R Liu, Q. Lu, Dalton Trans. 41 (2012) 5862-5868.

[8] (a) L. K. Das, A. Biswas, J. S. Kinyon, N. S. Dalal, H. Zhou, A. Ghosh, Inorg. Chem. 52 (2013) 11744-11757; (b) T. Chattopadhyay, M. Mukherjee, A. Mondal, P. Maity, A. Banerjee, K. S. Banu, S. Bhattacharya, B. Roy, D. J. Chattopadhyay, T. K. Mondal, M. Nethaji, E. Zangrando, D. Das, Inorg. Chem. 49 (2010) 3121-3129.

[9] (a) A. Panja, P. Guionneau, Dalton Trans. 42 (2013) 5068-5075; (b) S. Majumder, S. Sarkar, S. Sasmal, E. C. Sañudo, S. Mohanta, Inorg. Chem. 50 (2011) 7540-7554; (c) S. K. Mal, M. Mitra, G. Kaur, V. M. Manikandamathavan, M. S. Kiran, A. Roy Choudhury, B. U. Nair, R. Ghosh, RSC Adv. 4 (2014) 61337-61342.

[10] (a) S. Friedle, E. Reismer, S. J. Lippard, J. Chem. Soc. 39 (2010) 2768-2779; (b) P. C. A Bruijnincx, G. van Koten, R. J. M. K. Gebbink, Chem. Soc. Rev. 37 (2008) 2716-2744; (c) S. I. Chan, S. S. F. Yu, Acc. Chem. Res. 41 (2008) 969-979.

[11] R. Hage, A. Lienke, Angew Chem. Int. Ed. 45 (2005) 206-222; (b) N. Duran, E. Esposito, App. Catal. B 28 (2000) 83-99.

[12] L. Que, W. B. Tolman, Nature 455 (2008) 333-340.

[13] (a) N. C. Kasuga, K. Sekino, C. Koumo, N. Shimada, M. Ishikawa, K. Nomiya, J. Inorg. Biochem. 84 (2001) 55–65; (b) T. Rosu, M. Negoiu, S. Pasculescu, E. Pahontu, D. Poirier, A. Gulea, Eur. J. Med. Chem. 45 (2010) 774–781; (c) M. V. Angelusiu, S.-F. Barbuceanu, C. Draghici, G. L. Almajan Eur. J. Med. Chem. 45 (2010) 2055–2062.

[14] (a) K. Singh, M. Singh Barwa, P. Tyagi, Eur. J. Med. Chem. 41 (2006) 147–153; (b) K. Singh, M. Singh Barwa, P. Tyagi, Eur. J. Med. Chem. 42 (2007) 394-402; (c) G. B. Bagihalli, P. G. Avaji, S. A. Patil, P. S. Badami, Eur. J. Med. Chem. 43 (2008) 2639-2649; (d) S. A. Patil, V. H. Naik, A. D. Kulkarni, P. S. Badami, Spectrochim. Acta A 75 (2010) 347–354.

[15] M. G. Guzman, J. Dille, S. Godet, Int. J. Chem. Biomol. Eng. 2:3 (2009) 104-111.

[16] M. Karlsson, S. L. Oxberry, D. J. Hampson, Vet. Microbiol. 84 (2002) 123-133.

[17] R. Irkin, M. Korukluoglu, Afr. J. Biotechnol. 6 (2007) 384-387.

[18] O. O. Olajuyigbe, A. J. Afolayan, Molecules 17 (2012) 2103-2118.

[19] *CrystalClear 2.0*; Rigaku Corporation: Tokyo, Japan.

[20] G.M. Sheldrick, Acta Cryst. A64 (2008) 112-122.

[21] O.V. Dolomanov, L.J. Bourhis, R.J. Gildea, J.A.K. Howard, H. Puschmann, J. Appl. Crystallogr. 42 (2009) 339-341.

[22] L.J. Farrugia, 1998, ORTEP-32 for Windows. University of Glasgow, Scotland.

[23] K. Adwan, Abu-Hasan, Folia Microbiol. (1998) 438-440.

[24] J. Yao, R. Moellering, Antibacterial agents. In *Manual of Clinical Microbiology*; P. Murray, E. Baron, M. Pfaller, F. Tenover, R. Yolken (Eds); ASM Press: Washington, DC, USA, (1995) 1281-1290.

[25] F. Zippel, F. Ahlers, R. Werner, W. Haase, H.-F. Nolting, B. Krebs, Inorg. Chem. 35 (1996) 3409-3419.

[26] (a) A. I. Vogel, *Textbook of quantitative inorganic analysis, Longmans*, Green and Co. Ltd, London, 3rd edn, (1961) 366; (b) A. Neves, L. M. Rossi, A. J. Bortoluzzi, B. Szpoganicz, C. Wiezbicki and E. Schwingel, Inorg. Chem. 41 (2002) 1788-1794; (c) E.Monzani, L. Quinti, A. Perotti, L. Casella, M. Gullotti, L. Randaccio, S. Geremia, G. Nardin, P. Faleschini and G. Tabbi, Inorg. Chem. 37 (1998) 553-562.

Table 1. Crystal data and structure refinement parameters of **1** and **2**

Emperical formula	$C_{42}H_{39}N_6O_3S_3Co$ (**1**)	$C_{28}H_{26}N_4O_2S_2Ni$ (**2**)
Formula weight	830.90	573.38
T (K)	100	100
Wavelenght (Å)	0.71073	0.71073
Crystal system	Monoclinic	Monoclinic
Space group	$P2_1/n$	$P2_1/c$
Unit cell dimensions		
a (Å)	10.870(3)	5.1294 (8)
b (Å)	25.355(5)	9.9200 (17)
c (Å)	14.332(3)	24.111 (4)

α (°)	90	90
β (°)	102.257(7)	95.124 (10)
γ (°)	90	90
V (Å^3)	3859.8(14)	1222.0 (4)
Z	4	4
D_{calc} (Mg m^{-3})	1.430	1.558
Absorption coefficient (mm^{-1})	0.656	1.001
F(000)	1728	596
Crystal size (mm^3)	0.1 × 0.1 × 0.05	0.2 × 0.2 × 0.2
Theta range for data collection (°)	3.018-27.546	3.270-27.486
Index ranges	$-14 \le h \le 13$, $-32 \le k \le 24$, $-18 \le l \le 18$	$-6 \le h \le 6$, $-12 \le k \le 12$, $-31 \le l \le 31$
Reflections collected	24548	10477
Independent reflections	8815 [Rint= 0.0751]	2802 [Rint= 0.0969]
Completeness of theta	99.0 % [θ=25.242]	99.5 % [θ=25.242]
Absorption correction	Multi-scan	Multi-scan

T_{max} and T_{min}	1.000 and 0.897	1.000 and 0.796
Refinement method	Full matrix	Full matrix
Data/restrains/parameters	8815/0/ 496	2802/0/ 169
Goodness-of fit (GOF) F^2	1.049	1.069
Final R index [$l > 2\sigma(l)$]	R_1 = 0.0685 and wR_2 = 0.1381	R_1 = 0.0644 and wR_2 = 0.1253
R index (all data)	R_1 = 0.1112 and wR_2 = 0.1680	R_1 = 0.1040 and wR_2 = 0.1564
Largest difference between peak and hole (e Å^{-3})	0.768, -0.572	1.202, -0.488

Table 2. Bond lengths (Å) and bond angles (˚) data of **1**

Bond lengths			
Co(1)-O(1)	1.882(3)	Co(1)-N(1)	1.962(3)
Co(1)-O(2)	1.892(3)	Co(1)-N(2)	1.949(3)
Co(1)-O(3)	1.890(3)	Co(1)-N(3)	1.950(3)
Bond angles			
O(3)-Co(1)-O(2)	171.98(11)	O(1)-Co(1)-O(2)	86.75(12)
O(3)-Co(1)-N(2)	93.80(12)	O(1)-Co(1)-N(2)	171.29(12)

O(3)-Co(1)-N(1)	86.19(12)	O(1)-Co(1)-N(1)	94.10(12)
O(3)-Co(1)-N(3)	92.74(13)	O(1)-Co(1)-N(3)	84.18(12)
O(2)-Co(1)-N(2)	91.26(12)	N(2)-Co(1)-N(1)	94.27(13)
O(2)-Co(1)-N(1)	87.22(12)	N(2)-Co(1)-N(3)	87.49(13)
O(2)-Co(1)-N(3)	93.70(13)	N(3)-Co(1)-N(1)	178.00(13)
O(1)-Co(1)-O(3)	89.16(12)	O1 Co1 N2	171.29(12)

Table 3. Bond lengths (Å) and bond angles (˚) data of **2**

Bond lengths			
Ni(1)-O(1)	1.823(3)	Ni(1)-O(1')	1.823(3)
Ni(1)-N(1)	1.925(4)	Ni(1)-N(1')	1.925(4)
Bond angles			
O(1)-Ni(1)-N(1)	92.90(15)	O(1')-Ni(1)-N(1')	87.10(15)
O(1')-Ni(1)-N(1')	92.90(15)	O(1)-Ni(1)-O(1')	180.0
O(1)-Ni(1)-N(1)	87.10(15)	N(1)-Ni(1)-N(1')	180.0

Table 4. Zone of inhibition by the disc diffusion method for HL

Bacteria	Zone of Inhibition (mm)				
	HL			Cephotaxime (10 µg / Disc)	Ampicillin (10 µg / Disc)
	2.5 µg/ Disc	1µg/ Disc	0.1 µg/ Disc		
Bacillus Subtilis	13 ± 1.6	12 ± 1.4	12 ± 1.1	27 ± 1.8	18 ± 0.7
E.coli	12 ± 1	10 ± 1.2	10 ± 1.4	24 ± 0.8	10 ± 0.5

MIC (Minimum Inhibitory Concentration)

Concentrations tested: 100, 50, 25, 12.5, 6.25, 3.12, 1.56 µg / ml

Bacillus subtilis - 50 µg/ml, *E.coli* - 100 µg/ml

MBC (Minimum Bactericidal Concentration)

Concentrations tested: 100, 50, 25, 12.5, 6.25, 3.12, 1.56 µg / ml

Bacillus subtilis - 100 µg/ml; *E.coli* - > 100 µg/ml

Table 5. Zone of inhibition by the disc diffusion method for **1**

Bacteria	Zone of Inhibition (mm)				
	Compound **1**			Cephotaxime	Ampicillin
	2.5 µg/ Disc	1 µg/ Disc	0.1 µg/ Disc	10 µg / Disc	10 µg / Disc
Bacillus Subtilis	12	10	10	26	14
E.coli	10	10	-	19	14

MIC (Minimum Inhibitory Concentration)

Concentrations tested: 100, 50, 25, 12.5, 6.25, 3.12, 1.56 µg / ml

Bacillus subtilis - 50 µg/ml, *E.coli* - 100 µg/ml

MBC (Minimum Bactericidal Concentration)

Concentrations tested: 100, 50, 25, 12.5, 6.25, 3.12, 1.56 µg / ml

Bacillus subtilis - 100 µg/ml; *E.coli* - > 100 µg/ml

Table 6. Time kill assay for **1**

Bacteria	Log_{10} Kil							
	MIC				2 × MIC			
	0 h	4 h	8 h	12 h	0 h	4 h	8 h	12 h
E.coli	8.55	TNC[#]	TNC[#]	TNC[#]	8.45	TNC[#]	TNC[#]	TNC[#]
Bacillus subtilis	7.78	8.11	9.27	9.70	7.30	7.78	8.94	8.62

[#]TNC – Too numerous to count

Table 7. Zone of inhibition by the disc diffusion method for **2**

Bacteria	Zone of Inhibition (mm)				
	Compound **2**			Cephotaxime (10 µg / Disc)	Ampicillin (10 µg / Disc)
	2.5 µg/ Disc	1 µg/ Disc	0.1 µg/ Disc		
Bacillus Subtilis	15.5 ± 1.3	15.3 ± 1.5	12.6 ± 1.1	25.3 ± 1.1	17.3 ± 0.6
E.coli	11 ± 1	10.25 ± 1.2	8.3 ± 1.5	25.3 ± 0.5	19 ± 1

MIC (Minimum Inhibitory Concentration)

Concentration tested: 100, 50, 25, 12.5, 6.25, 3.12, 1.56 µg/ml

E.coli – 25 µg/ml, *Bacillus Subtilis* – 12.5 µg/ml

MBC (Minimum Bactericidal Concentration)

Concentration tested: 100, 50, 25, 12.5, 6.25, 3.12, 1.56 µg/ml

E.coli – 50 µg/ml, *Bacillus Subtilis* – 25 µg/ml

Table 8. Time kill assay for **2**

Bacteria	Log_{10} Kil							
	MIC				2 × MIC			
	0 h	4 h	8 h	12 h	0 h	4 h	8 h	12 h
E. coli	9.344	TNC[#]	TNC[#]	TNC[#]	9.060	9.170	TNC[#]	9.465
Bacillus subtilis	9.025	8.710	8.570	7.470	NG[§]	NG[§]	NG[§]	NG[§]

[#]TNC – Too numerous to count; [§]NG – No growth

Table 9. Kinetic parameters for the oxidation of 3,5-DTBC catalyzed by **1** and **2**

Solvent	Compounds	V_{max} (M s^{-1})	Std. error	K_M (M)	Std. error	K_{cat} (h^{-1})
MeOH	**1**	9.65×10^{-5}	4.19×10^{-5}	7.59×10^{-3}	4.54×10^{-3}	3.47×10^{3}
MeOH	**2**	7.45×10^{-5}	4.91×10^{-5}	4.02×10^{-3}	1.99×10^{-3}	2.68×10^{3}

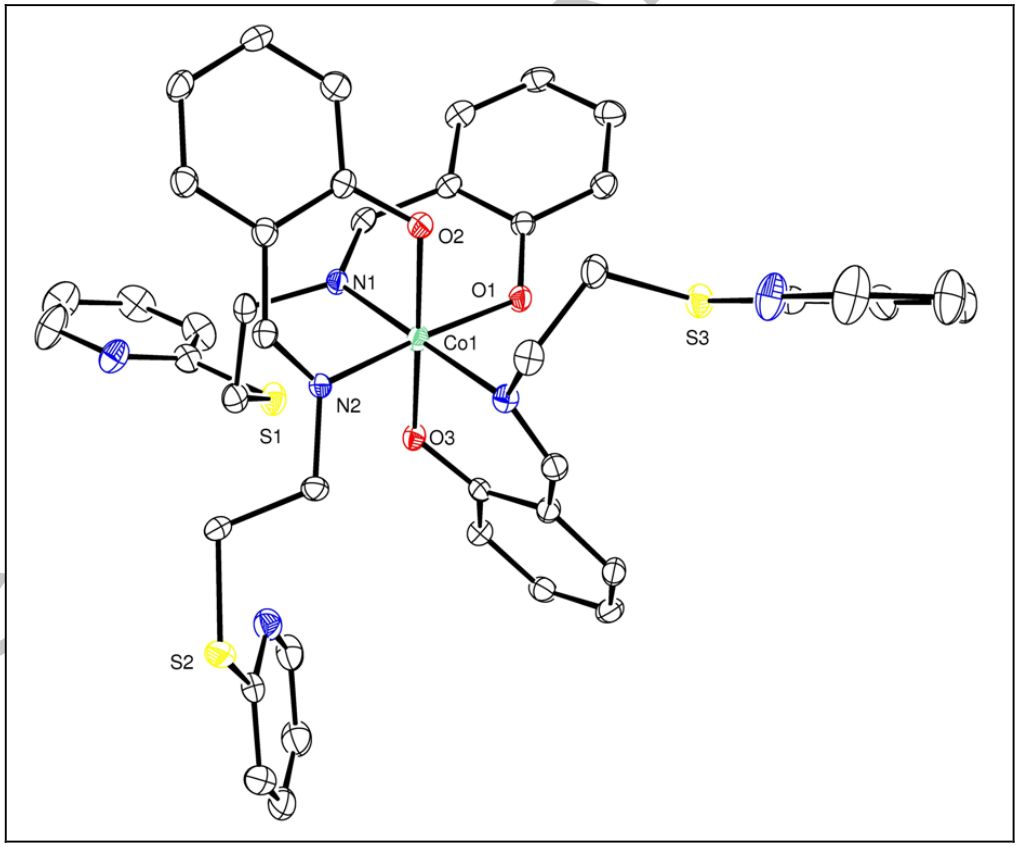

Fig. 1. ORTEP of **1** with 30% ellipsoid probability plot (H atoms are excluded for clarity)

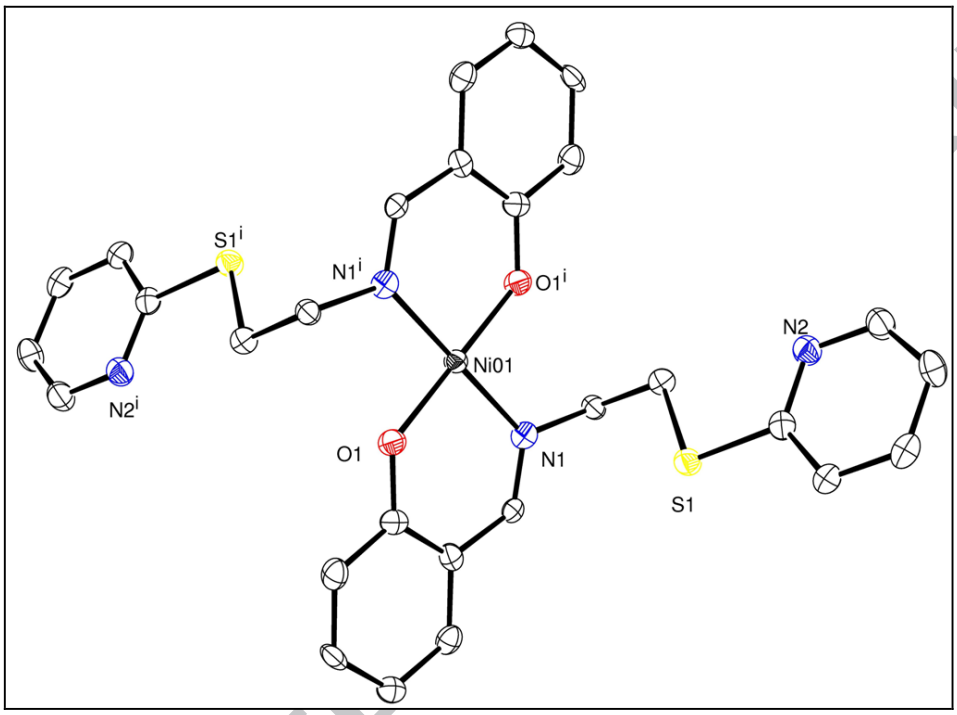

Fig. 2. ORTEP of **2** with 30% ellipsoid probability plot (H atoms are excluded for clarity)

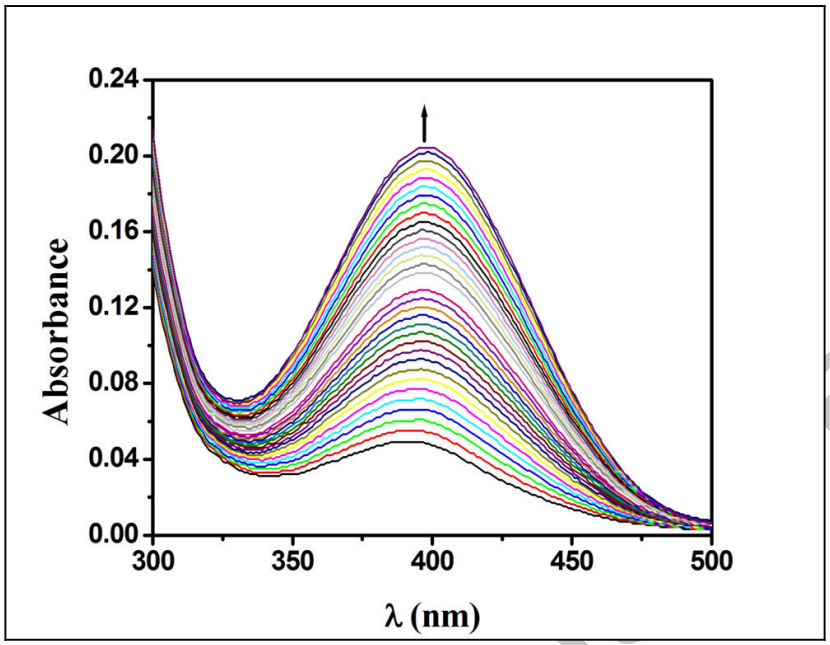

Fig. 3. Change in the spectral pattern of 3,5-DTBC in the presence of **1** in MeOH, observing the reaction for 4 h; inset: spectrum of pure 3,5-DTBC in MeOH

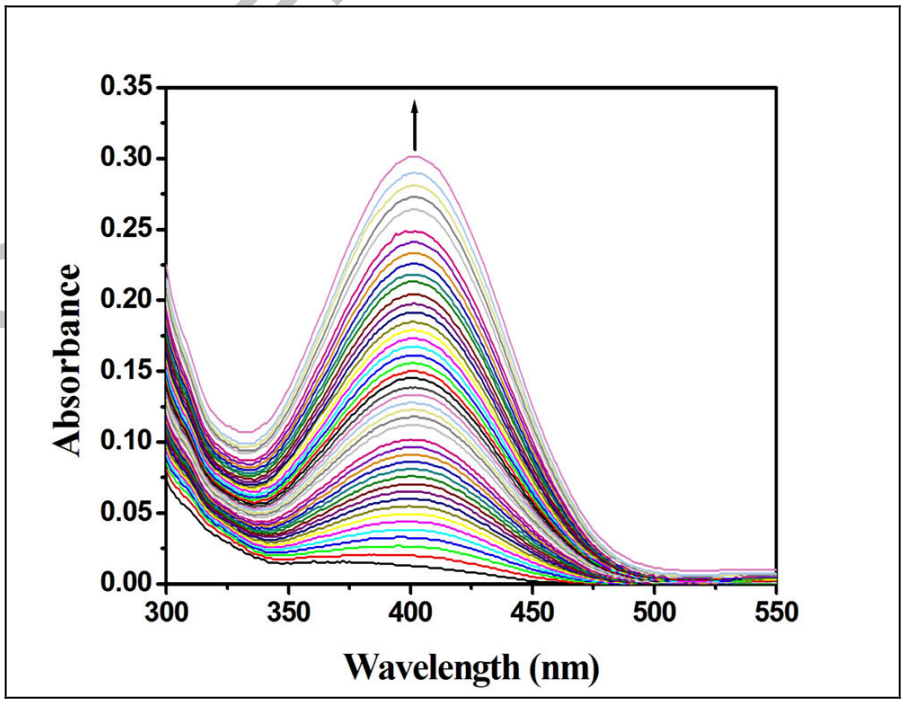

Fig. 4. Change in the spectral pattern of 3,5-DTBC in the presence of **2** in methanol, observing the reaction for 4 h

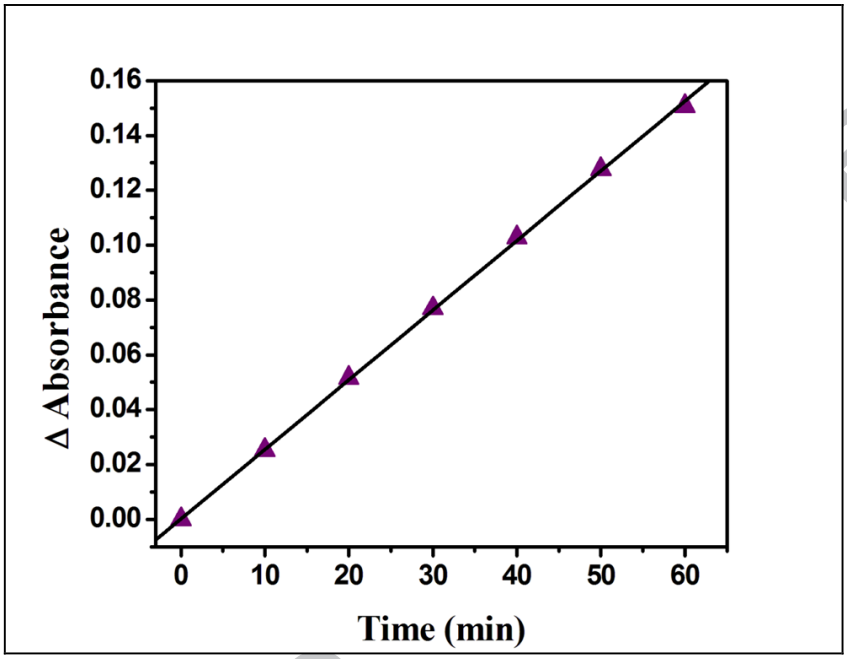

Fig. 5. A plot of the difference in absorbance (ΔA) vs time to evaluate the velocity of the catalytic oxidation of 3,5-DTBC by **1** in MeOH

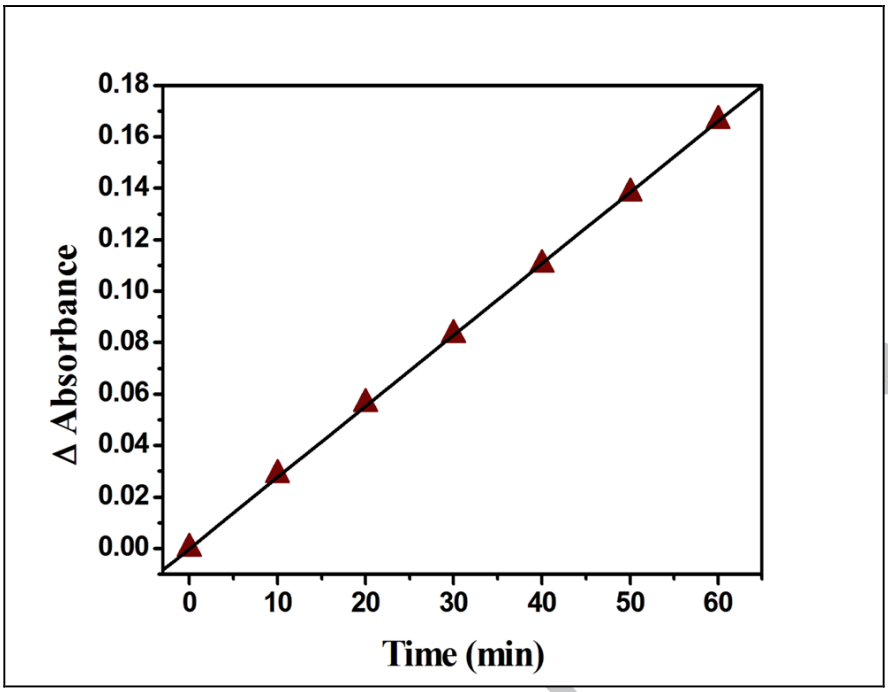

Fig. 6. A plot of the difference in absorbance (ΔA) vs time to evaluate the velocity of the catalytic oxidation of 3,5-DTBC by **2** in MeOH

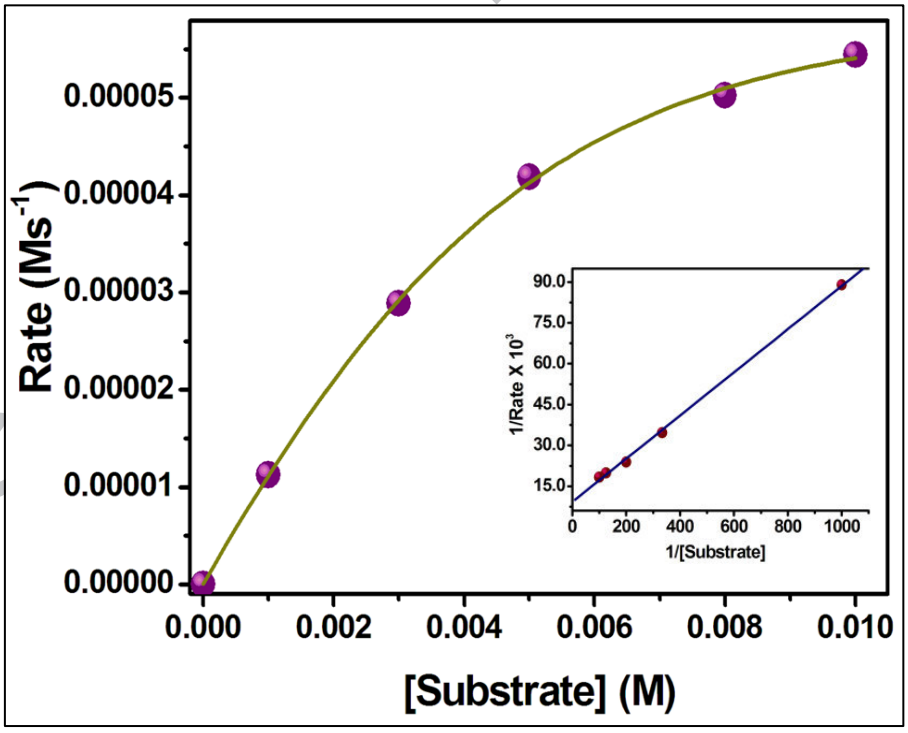

Fig. 7. Plot of rate vs. [substrate] in the presence of **1** in MeOH; inset: Lineweaver-Burk plot.

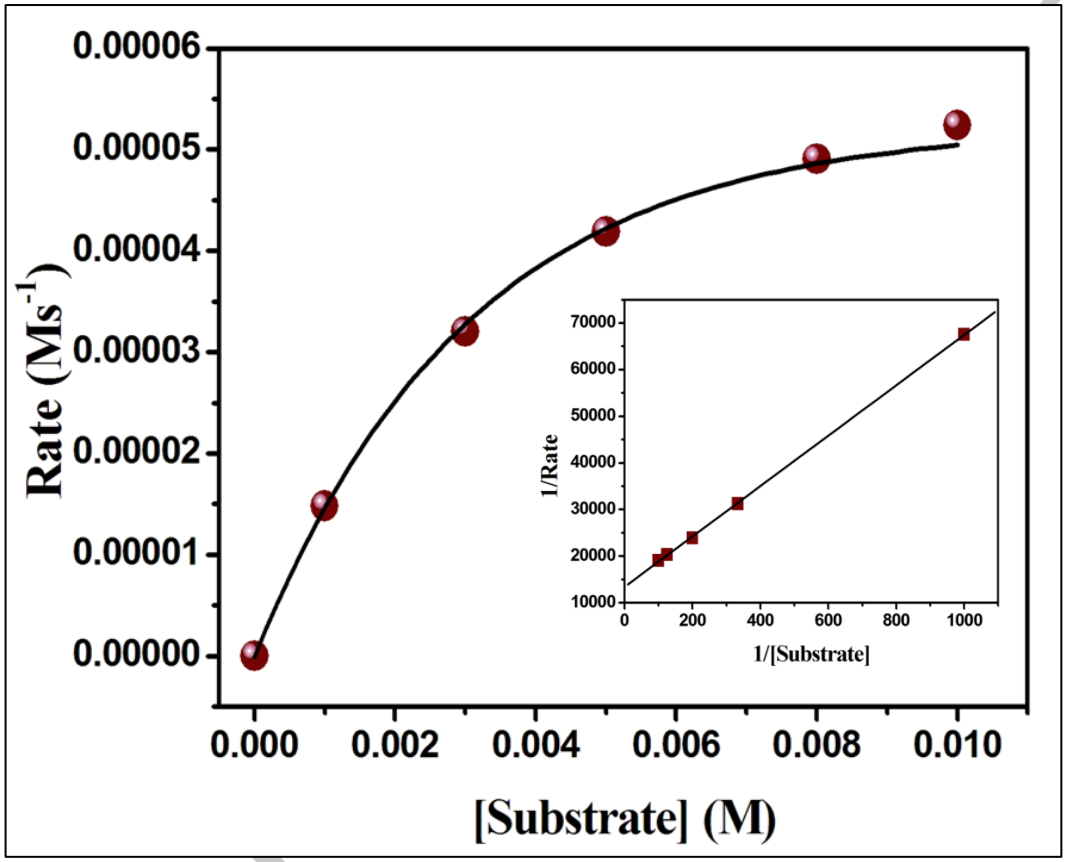

Fig. 8. Plot of rate vs. [substrate] in the presence of **2** in MeOH; inset: Lineweaver-Burk plot.

Antibacterial and catecholase activities of Co(III) and Ni(II) Schiff base complexes

Ayon Kanti Ghosh, Merry Mitra, Aafreen Fathima, Hareram Yadav, Angshuman Roy Choudhury, Balachandran Unni Nair*, Rajarshi Ghosh*